ANALYSIS OF ACOUSTIC-VIBRATION SIGNALS OF AMORPHOUS ALLOY THREE-DIMENSIONAL COILED CORE TRANSFORMERS AND ITS CONDITION ASSESSMENT

Xinxin Chen[1], Yuhui Chen[2], Junsong Li[1], Tao Zhao[3], Rui Zhu[3*]
[1]Shantou Power Supply Bureau of Guangdong Power Grid Co., Ltd., Shantou 515000, China
[2]Guangzhou Power Supply Bureau of Guangdong Power Grid Co., Ltd., Guangzhou 510630, China
[3]Hebei Provincial Key Laboratory of Power Transmission Equipment Security Defense (North China Electric Power University), Baoding 071003, China

Abstract - Transformer acoustic and vibration signals can reflect internal mechanical conditions, thereby enabling early warning of typical abnormalities. Because amorphous-alloy three-dimensional wound-core transformers differ substantially from conventional transformers in both core material and structure, their acoustic and vibration characteristics are also distinct. This study investigates the first 110 kV amorphous-alloy three-dimensional wound-core power transformer deployed in China and performs acoustic and vibration signal acquisition and statistical analysis of the characteristic quantities. Signals collected from the core surface and metal tank wall were analysed to determine the distributions of five characteristic quantities: dominant frequency, fundamental-frequency proportion, high-to-low frequency ratio, odd-to-even harmonic ratio, and mean autocorrelation degree. These distributions were then compared with those reported for conventional power transformers. Under the investigated normal operating conditions, the dominant frequencies were concentrated at 200 and 300 Hz. The preliminary odd-to-even harmonic-ratio intervals were [0.033, 0.204] for vibration signals and [0.043, 0.379] for acoustic signals, whereas the corresponding high-to-low frequency-ratio intervals were [0.138, 0.612] and [0.217, 0.613], respectively. The core-surface vibration characteristics were more concentrated than those measured on the tank wall, and the overall distributions obtained from the factory and field measurements were broadly consistent. Comparison with conventional silicon-steel transformers revealed material- and structure-specific characteristic distributions. The reported intervals should be regarded as preliminary baseline references rather than universal diagnostic thresholds and provide a basis for subsequent validation involving multiple units and fault conditions.

Keywords: Amorphous alloy, Power transformer, Acoustic and vibration signal acquisition, Characteristic-quantity analysis, Characteristic distributions.

1. Introduction

To support China's “dual-carbon” objectives, the deployment of high-efficiency, energy-saving transformers has become increasingly important. Transformers are essential components of power systems, and their operational efficiency and safety directly affect the economical and reliable operation of the power grid. In China, transformer losses account for more than 4% of total electricity generation and approximately 30% of distribution-network losses [1-3].
Given the substantial energy-saving potential of amorphous-alloy transformers, utilities and manufacturers are actively promoting their application. Compared with silicon-steel transformers, transformers employing amorphous-alloy exhibit lower no-load losses and are therefore attractive for energy-efficiency improvements in distribution networks [4-7].

Li et al. reported that DC bias significantly affects the direction and symmetry of magnetostriction in three-phase five-limb transformers [8]. Compared with conventional three-phase five-limb amorphous-alloy cores, three-dimensional wound-core structures have fully symmetrical magnetic circuits and triangular core arrangements, providing enhanced structural stability and short-circuit

dx.doi.org/10.17683/ijomam/issue25/v1.25

withstand capability [9]. However, ferromagnetic materials undergo dimensional changes under magnetic excitation, and amorphous alloys generally exhibit greater magnetostriction than conventional silicon steel, resulting in higher vibration and associated noise levels [10]. Experimental investigations [11] and numerical simulations [12] have confirmed that core magnetostriction is a principal source of transformer vibration and noise, providing a basis for vibration- and noise-mitigation studies.

Acoustic and vibration signals can also reflect the internal mechanical condition of a transformer and facilitate early warning of typical mechanical faults. Acoustic-vibration monitoring and diagnostic techniques for conventional silicon-steel transformers have developed rapidly [13]. Vibro-acoustic monitoring has been applied to the assessment of transformer mechanical condition, winding deformation, core looseness, and excitation abnormalities [14-17]. Miao et al. [18] developed an electromagnetic-mechanical-acoustic finite-element model for a 220 kV oil-immersed power transformer and validated the coupled prediction of structural vibration and radiated noise through product-level tests under the investigated operating conditions. Song et al. [9] investigated a 200 kVA amorphous-alloy three-dimensional wound-core prototype using a magneto-mechanical coupling model and vibration measurements, thereby identifying the vibration distribution and dominant-frequency characteristics of the wound core. Liu et al. [19] further examined a 50 kVA amorphous-alloy three-dimensional wound-core transformer through magnetostriction measurements, coupled simulations, vibration and noise experiments, and clamping-force analysis. Their results showed that clamping force exerted a nonlinear influence on core vibration. Chen et al. [20] combined coupled acoustic-vibration simulations with controlled experiments on a magnetically controlled dry-type distribution transformer and found that DC bias increased both vibration and noise while enhancing the odd-order harmonic content.

Research on the acquisition and characteristic analysis of acoustic and vibration signals from amorphous-alloy three-dimensional wound-core power transformers remains limited. The present study investigates a 110 kV amorphous-alloy three-dimensional wound-core transformer through acoustic and vibration signal acquisition and statistical analysis. Signals were collected from both the core surface and the metal tank wall, and their characteristic distributions were compared with those of conventional transformers. The results provide a technical basis for optimizing measurement-point arrangements for amorphous-alloy three-dimensional wound-core power transformers and for understanding the characteristic distributions and engineering applications of their acoustic and vibration signals.

2. Test Setup and Methods

2.1 Test Object

The test object was a 110 kV energy-saving amorphous-alloy three-dimensional wound-core transformer. Figure 1 shows the transformer core and the fully assembled transformer before factory delivery.

(a) Transformer core (b) Transformer body

Figure 1: Three-dimensional wound core and amorphous-alloy strip material

The main technical parameters are summarized in Table 1.

Table 1. Main technical parameters of the test transformer

Parameter	Unit	Specification
Model	/	SZH25-RL-20000/110-NX1
Rated capacity	kVA	20000
Rated voltage	kV	110/11
Connection group	/	YNd11
Frequency	Hz	50
Phase	/	3
No-load loss	/	≤4.24
Load loss	/	≤75.00
Total loss	/	≤79.24
Impedance	%	16

An SR-TVA2019-A acoustic-vibration monitoring device was used, and its principal parameters are listed in Table 2.

Table 2. Main parameters for acoustic and vibration monitoring

	Parameter	Value
Acoustic monitoring	Dynamic range	38 dB-110 dB
	Frequency range	20 Hz-20 kHz
	Audio sampling rate	32,768 Hz
	Maximum sound-pressure level	120 dB
	Sensitivity	-26 dB
Vibration monitoring	Vibration-acceleration range	±10 g
	Resonant frequency	21 kHz
	3 dB bandwidth	11 kHz
	Signal sampling rate	32,768 Hz
	Output sensitivity	200 mV/g

2.2 Test Methods

Acoustic and vibration signals were acquired both before factory delivery and during field operation. During the factory tests, vibration signals were measured directly on the core surface, while acoustic signals were measured in the adjacent sound field. During the factory acceptance and field tests, signals were collected from the transformer tank wall and the surrounding sound field. The factory tests were conducted under rated no-load conditions, whereas the field measurements were performed under light-load conditions, with an average load factor of approximately 14%.

Figure 2 schematically illustrates the acoustic and vibration measurement points on the transformer core. The vibration-acceleration sensors were attached to the surface of the upper core yoke at positions ①-⑤, arranged from left to right.

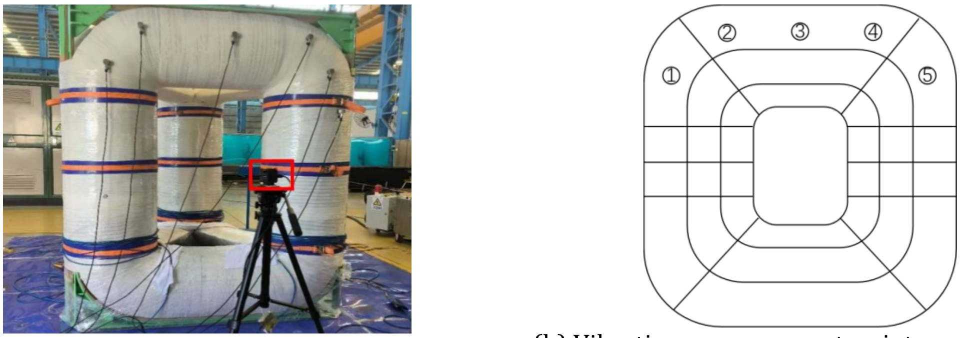

(a) Acoustic measurement-point arrangement (b) Vibration measurement-point arrangement

Figure 2: Core measurement-point arrangement

Figure 3 schematically illustrates the acoustic and vibration measurement points used during the transformer factory test. The acoustic sensor was positioned 1.8 m from the transformer tank-wall at a height of 2.5 m, and the vibration sensors were installed on the high-voltage bushing side at positions ①-⑥.

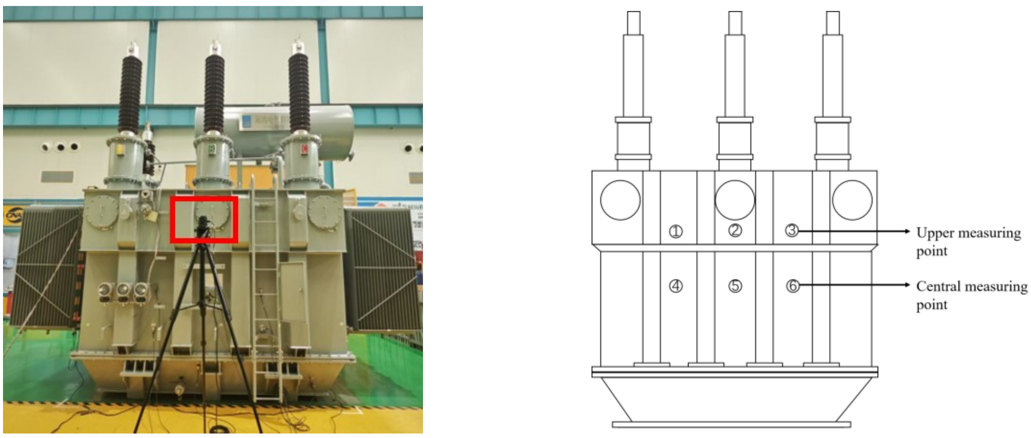

(a) Acoustic measurement-point arrangement (b) Vibration measurement-point arrangement

Figure 3: Tank-wall measurement-point arrangement

Figure 4 shows the arrangement of the acoustic and vibration measurement points after the transformer was commissioned at a 110 kV substation. The field arrangement was consistent with that used during the factory tests.

Figure 4: Field measurement-point arrangement

2.3 Calculation of Signal Characteristic Quantities

Time-domain acoustic and vibration signals were collected from the transformer core and tank-wall under rated-voltage no-load and light-load conditions. The signals were transformed into the frequency domain using the Fourier transform. The following characteristic quantities were analysed [21]:

1) Dominant Frequency:

The dominant frequency is the frequency associated with the maximum signal power spectral density and is an important quantity for signal-feature extraction. After the time-domain signal is transformed using the Fourier transform, the corresponding time-domain waveform and frequency-amplitude spectrum are obtained, as illustrated in Figure 5. The frequency component with the maximum amplitude in the spectrum is identified as the dominant frequency; in the example shown, the dominant frequency is 200 Hz.

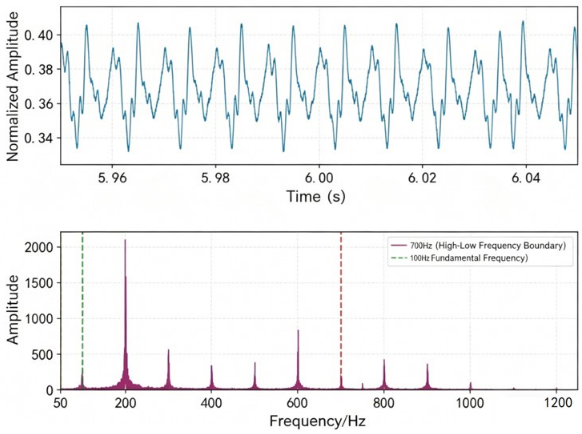

Figure 5: Example time-domain waveform and frequency spectrum

2) 50 Hz Odd-to-Even Harmonic Ratio:

$$R_{\text{oe}} = \frac{\sum_{f_{\text{odd}}=50}^{1950} X(f_{\text{odd}})}{\sum_{f_{\text{even}}=100}^{2000} X(f_{\text{even}})} \tag{1}$$

$X(f)$ denotes the amplitude at frequency f in the signal spectrum. Here, f_{odd} and f_{even} denote the odd- and even-harmonic frequency components, respectively, of the rated frequency of 50 Hz, with an upper frequency limit of 2,000 Hz. The odd-to-even harmonic ratio characterizes the ratio of the odd harmonics (50, 150, 250 Hz, etc.) to the even harmonics (100, 200, 300 Hz, etc.) in the signal spectrum.

3) High-to-Low Frequency Ratio:

$$R_{\text{hl}} = \frac{\sum_{f=f_h}^{2000} X(f)}{\sum_{f=50}^{f_h} X(f)} \tag{2}$$

f_h denotes the boundary between the high- and low-frequency bands and was set to 700 Hz in this study.

4) Fundamental-Frequency Proportion:

The fundamental-frequency proportion represents the contribution of the winding-vibration fundamental frequency to the total energy of the acoustic or vibration signal spectrum. It is calculated as follows:

$$P_{f_0} = X^2(f_0) / \sum_{f=f_0}^{2000} X^2(f) \tag{3}$$

f_0 denotes the fundamental frequency, which is 100 Hz for vibration induced by a 50 Hz power-frequency supply.

5) Mean Autocorrelation Degree:

$$d = \sum_{m=2}^{m_{\max}} R_{\text{rel}}(m) / (m_{\max} - 1) \tag{4}$$

Here, m is the time-frame index, m_{max} is the total number of time frames into which a segment of the acoustic signal is divided, and R_{rel} is the correlation coefficient between $X(m)$ and $X(m-1)$.

The mean autocorrelation degree d primarily reflects temporal variations in the signal spectrum. Under normal operating conditions, the spectral characteristics of a transformer are generally stable. After the short-time Fourier transform (STFT) is applied to an acoustic or vibration signal, the spectra of adjacent time frames differ only slightly and therefore exhibit a high correlation. By contrast, a transformer with loose components may exhibit non-stationary behaviour, resulting in pronounced spectral variations between adjacent time frames and a reduced correlation. This quantity can therefore be used to characterize unstable operating conditions.

3. Test Results and Analysis

3.1 Statistical Analysis Method

To compare the distributions, dispersion, and central tendencies of the characteristic quantities obtained under different test scenarios and at different measurement points, box plots were used for visual analysis. The principal components of a box plot are illustrated in Figure 6.

The lower and upper boundaries of the box represent the first quartile (Q1) and third quartile (Q3), respectively. The box spans the interquartile range (IQR = Q3 - Q1), which contains the central 50% of the sample data. The solid line within the box represents the median, whereas the dashed line represents the mean.

The upper and lower whiskers indicate the upper and lower limits of the non-outlying data, corresponding to Q3 + 1.5IQR and Q1 - 1.5IQR, respectively.

Data points outside the whiskers are classified as outliers because they lie beyond the 1.5IQR limits.

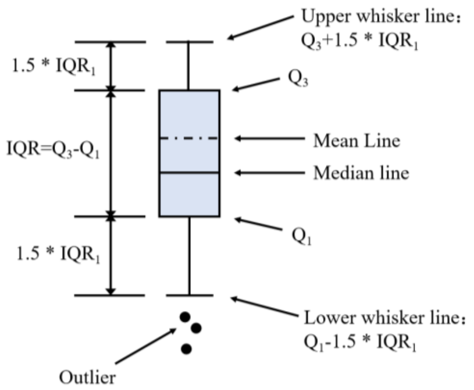

Figure 6: Components of a box plot

For the two factory-test scenarios, namely the bare core and the transformer tank-wall, 100 signal samples were collected and processed at each measurement point. The characteristic quantities were calculated from these samples using the procedures described in Section 2.3, after which box plots were constructed. Compared with conventional line and bar charts, box plots clearly display differences in data distribution, dispersion, stability, and outliers without requiring an assumption of normality. They therefore provide intuitive visual support for evaluating the effectiveness and consistency of each characteristic quantity and its relationship with the operating condition.

3.2 Statistical Analysis of Characteristic Quantities

3.2.1 Core and Tank-Wall Measurements

The acoustic and vibration characteristic quantities measured on the transformer core and at the corresponding tank-wall positions during the factory tests were statistically analysed, and the resulting box plots are shown in Figures 7 and 8. On the horizontal axes, core measurement points ①-⑤ correspond to the five positions arranged from left to right on the upper yoke in Figure 2(b), whereas tank-wall measurement points ①-③ correspond to the three upper positions arranged from left to right in Figure 3(b). The characteristic quantities obtained at corresponding core and tank-wall positions were then compared.

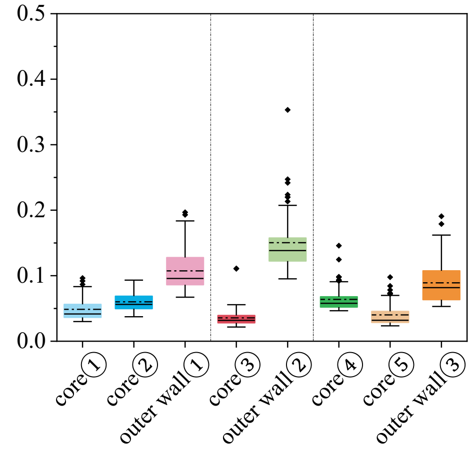

(a) 50 Hz Odd-to-Even Harmonic Ratio

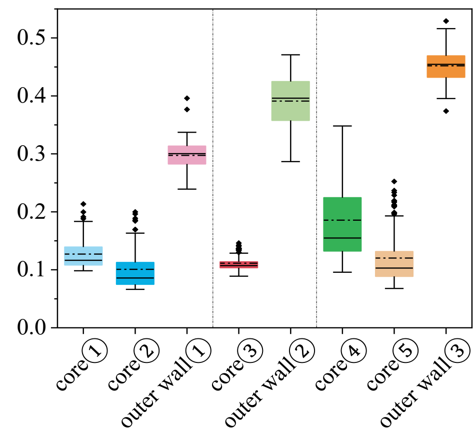

(b) High-to-Low Frequency Ratio

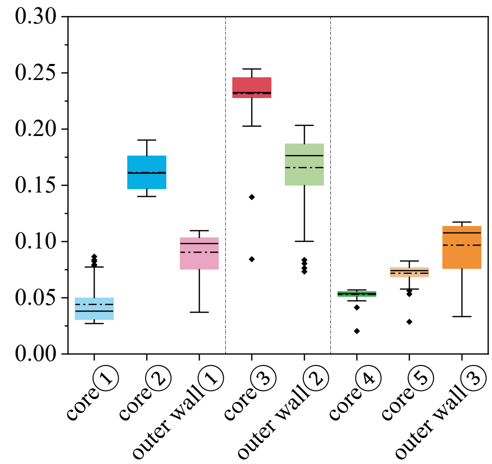

(c) Fundamental-Frequency Proportion

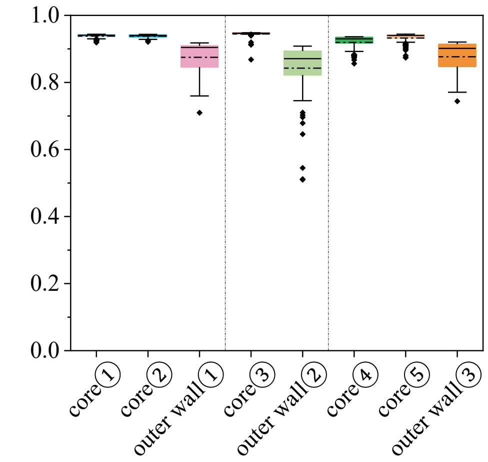

(d) Mean Autocorrelation Degree

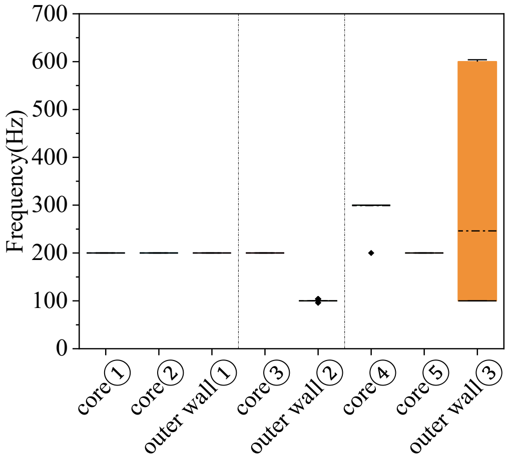

(e) Dominant Frequency

Figure 7: Box plots of vibration characteristic quantities at the measurement points

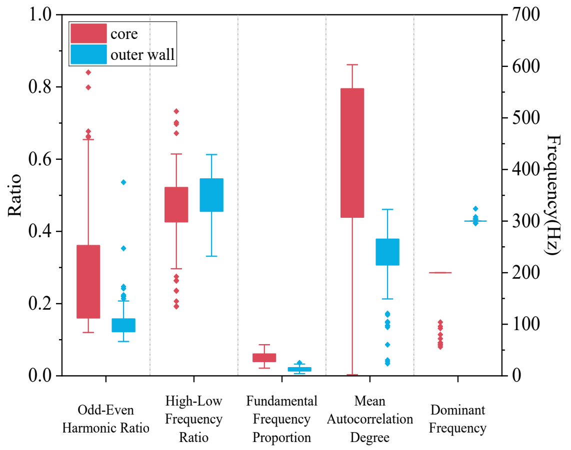

Figure 8: Box plots of acoustic characteristic quantities at the core and tank wall

Figure 7 presents box plots of the vibration characteristic quantities measured on the core and tank wall. Figure 7(a) shows that the 50 Hz odd-to-even harmonic ratios at all core measurement points were lower than those at the tank-wall measurement points. The boxes for the core measurements were relatively short, with non-outlying interquartile ranges primarily within 0-0.08, indicating that the samples were highly concentrated. By contrast, the boxes for the tank-wall measurements were longer, with interquartile ranges of approximately 0.05-0.15 and more dispersed samples. These results indicate that the insulating oil and intervening structural components between the core and tank wall affect vibration transmission and broaden the distribution of the 50 Hz odd-to-even harmonic ratio.

Figure 7(b) shows that the high-to-low frequency ratio was generally lower at the core measurement points and higher at the tank-wall measurement points, with differences of approximately 0.2-0.3. This trend indicates a degree of consistency between the corresponding internal and external measurement positions. A lower ratio indicates a greater contribution from low-frequency components and weaker high-frequency disturbances, consistent with the low-frequency-dominant nature of the signals.

The fundamental-frequency proportions shown in Figure 7(c) exhibit relatively large dispersion. Nevertheless, a positive relationship is apparent between the core measurement points and the corresponding adjacent tank-wall points: positions with higher fundamental-frequency proportions on the core generally correspond to higher values on the adjacent tank wall.

As shown in Figure 7(d), the mean autocorrelation degrees at all core-surface measurement points (①-⑤) were highly concentrated within 0.92-0.95. The boxes were very short, and the mean and median lines nearly coincided, indicating strong signal consistency. The corresponding tank-wall values (points ①-③) were distributed within 0.75-0.90. The differences between corresponding core-surface and tank-wall measurements remained relatively stable at approximately 0.10-0.15, suggesting that the attenuation of signal periodicity through the tank structure was comparatively stable. However, the longer boxes for the tank-wall points indicate greater signal dispersion.

Figure 7(e) shows that the dominant vibration frequencies at the core-surface measurement points were primarily 200 and 300 Hz. The dominant frequencies measured on the tank wall were more dispersed, particularly at tank-wall point ③, where some samples exhibited a dominant frequency of 600 Hz; however, the sample mean remained within 200-300 Hz.

These results indicate that measurements on the core surface directly capture the original vibration generated by magnetostriction. Under power-frequency magnetic excitation, these signals exhibit high regularity, low randomness, and relatively few high-frequency components. Consequently, they are characterized by concentrated mean autocorrelation degrees, low odd-to-even harmonic and high-to-low frequency ratios, and concentrated dominant frequencies. By contrast, tank-wall vibration signals propagate through multiple media, including the core, clamps and insulation, transformer oil, and tank wall. Differences in transmission paths, assembly tolerances, and other factors increase signal dispersion, resulting in more dispersed dominant frequencies and higher odd-to-even harmonic and high-to-low frequency ratios at the tank-wall measurement points.

Figure 8 presents box plots of the acoustic characteristic quantities measured for the bare core and the assembled transformer. For the bare-core measurements, the boxes were generally longer and covered wider ranges, whereas the characteristic quantities measured from the assembled transformer were more concentrated. Among the quantities considered, the high-to-low frequency ratio showed the greatest overlap between the two scenarios, indicating that transmission through the enclosure did not substantially alter the overall balance between the high- and low-frequency components. The other characteristic quantities differed more clearly between the two scenarios. When the bare-core acoustic signals were measured, the core was not strongly constrained by the tank, clamps, or compression structures, resulting in larger fluctuations and wider distributions. In the assembled transformer, the core was constrained by the clamps, tank, insulation, and compression structures. The acoustic signals radiated into the air only after attenuation and equalization through these structures, the transformer oil, and the tank, resulting in more concentrated and stable distributions.

3.2.2 Vibration Characteristics at Different Tank-Wall Measurement Points During Factory Testing

The preceding results show that the signal characteristics also vary among different positions on the transformer tank wall. In this section, box plots are used to compare the vibration characteristic quantities obtained at the six tank-wall measurement points used during the factory test, as illustrated in Figure 3(b). The results are presented in Figure 9.

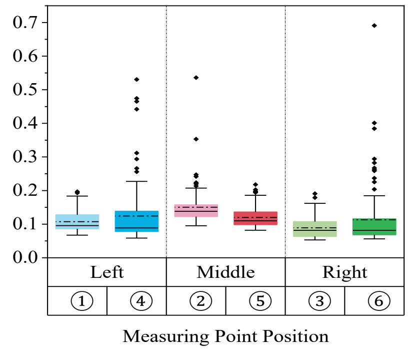

(a) 50 Hz Odd-to-Even Harmonic Ratio

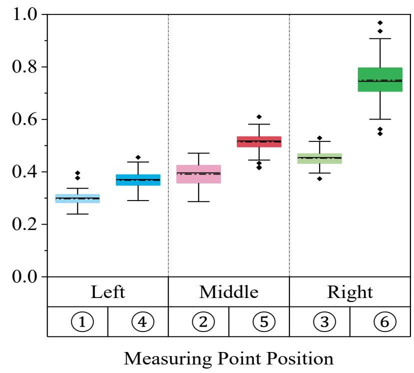

(b) High-to-Low Frequency Ratio

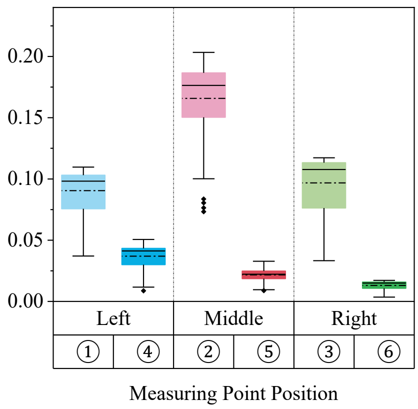

(c) Fundamental-Frequency Proportion

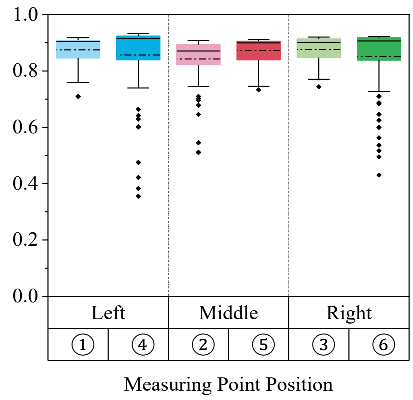

(d) Mean Autocorrelation Degree

Figure 9: Box plots of characteristic quantities at the tank-wall measurement points

Figure 9(a) presents the 50 Hz odd-to-even harmonic ratios. The distributions for point pairs ① and ④, ② and ⑤, and ③ and ⑥ overlap substantially and are generally concentrated, indicating good consistency between measurement points in the same column. The high-to-low frequency ratios in Figure 9(b) also exhibit a positive relationship within each column; that is, the upper and adjacent lower measurement points show similar trends. Figure 9(c) reveals a comparable positive relationship for the fundamental-frequency proportion, whereby a high value at an upper point corresponds to a high value at the middle point in the same column, consistent with the approximately linear transmission of vibration. As shown in Figure 9(d), the mean autocorrelation degrees at all points were mainly distributed between 0.80 and 0.95, and the box plots overlapped substantially, indicating strong consistency among signals measured at different positions.

In summary, although the vibration characteristics differed slightly among the six tank-wall measurement points, the differences were small and the overall consistency was good. Characteristic quantities measured at points in the same column exhibited similar magnitudes or synchronous variation. This relationship may therefore be used to optimize the number and placement of vibration sensors.

3.2.3 Field Acoustic and Vibration Signal Analysis

After the transformer was commissioned, box plots were constructed for the characteristic quantities of the tank-wall vibration signals and acoustic signals obtained from field measurements, as shown in Figure 10. Because the vibration signals from the six field measurement points exhibited a high degree of consistency, Figure 10 presents the statistical results obtained by combining the signals from all six points.

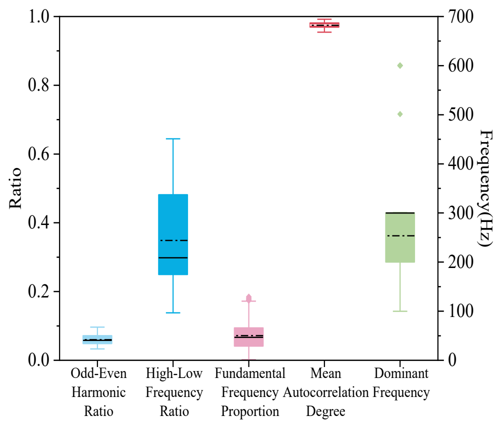

(a) Vibration signal

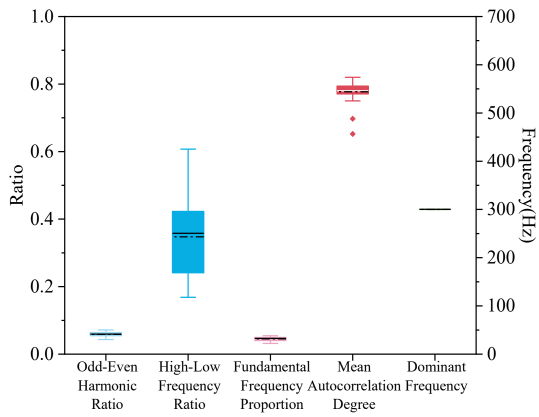

(b) Acoustic signal

Figure 10: Box plots of characteristic quantities obtained from field measurements

Based on the results presented in Section 3.2.2, the acoustic and vibration characteristic quantities obtained under the factory and field scenarios were compared. The box-plot ranges obtained from the field measurements were generally consistent with those from the factory tests.

The vibration consistency associated with the symmetry of the core structure was maintained during field operation, indicating that no obvious structural deformation occurred after commissioning.

Table 3 compares the distribution ranges of the vibration characteristic quantities before and after factory delivery.

Table 3. Comparison of vibration characteristic quantities before and after factory delivery

Characteristic quantity	In-plant vibration samples	Field vibration samples
Odd-to-even harmonic ratio	[0.033, 0.097]	[0.035, 0.204]
High-to-low frequency ratio	[0.138, 0.612]	[0.194, 0.613]
Fundamental-frequency proportion	[0.002, 0.172]	[0.006, 0.055]
Mean autocorrelation degree	[0.954, 0.992]	[0.741, 0.933]

The high-to-low frequency ratio obtained from the field measurement points covered a slightly wider range than that obtained during the factory tests. Two factors may account for this difference. First, ambient noise and vibration from other substation equipment may have slightly increased the dispersion of the high-to-low frequency ratio. Second, the winding load current may have contributed to the difference. Although the transformer operated at a low load factor during the field measurements, the electromagnetic forces acting on the windings increased the vibration and signal complexity.

The mean autocorrelation degree remained high under both test conditions, although the field distribution was broader than the in-plant distribution. The odd-to-even harmonic ratio and fundamental-frequency proportion showed no substantial changes relative to the factory-test results, indicating that the transformer excitation state and vibration-transmission characteristics remained broadly consistent after field commissioning.

The dominant frequencies of the field acoustic and vibration signals were 200 and 300 Hz, and no systematic dominant-frequency shift or distortion was observed. This result is consistent with the inherent vibration characteristics dominated by even-order harmonics. No measurement point exhibited an abnormal persistent dominant frequency above 300 Hz, indicating that the transformer showed no evident excitation abnormality or structural deformation during the investigated field operation and that the signals provide useful baseline information.

The field measurements confirmed the acoustic and vibration characteristics observed during the factory tests. Environmental noise, vibration from other substation equipment, and background interference from power-system operation produced only minor changes in signal amplitude and dispersion and introduced a small amount of high-frequency interference, without altering the principal frequency characteristics or periodicity. No abrupt amplitude changes or systematic frequency deviations were observed at any measurement point. These findings indicate that external constraints and interference had a limited effect on the principal acoustic and vibration characteristics of this transformer type and mainly influenced signal amplitude and dispersion.

3.3 Comparison with Conventional Power Transformers

Reference [22] reports a statistical analysis of test samples from 162 conventional-core power transformers and provides the principal distribution intervals of acoustic characteristic quantities under steady-state operation. In the present study, distribution ranges were obtained from acoustic and vibration samples collected before factory delivery and after grid-connected operation and were compared with the results reported in Reference [22], as shown in Table 4.

Table 4. Comparison of preliminary reference intervals for characteristic quantities

Characteristic quantity	Vibration samples in this study	Acoustic samples in this study	Conventional-transformer acoustic samples [22]
Odd-to-even harmonic ratio	[0.033, 0.204]	[0.043, 0.379]	[0.015, 0.852]
High-to-low frequency ratio	[0.138, 0.612]	[0.217, 0.613]	[0.0134, 0.1366]
Fundamental-frequency proportion	[0.002, 0.189]	[0.006, 0.055]	[0.025, 0.455]
Mean autocorrelation degree	[0.741, 0.992]	[0.75, 0.82]	[0.9775, 1]

As shown in Table 4, the preliminary intervals of the 50 Hz odd-to-even harmonic ratio for the acoustic and vibration samples in this study are considerably narrower than those reported for conventional-core transformers and have substantially lower upper limits. This result is consistent with the steady-state vibration characteristics of this transformer type, which are dominated by even-order harmonics. The narrow intervals and low upper limits indicate stable harmonic characteristics. A measured value above the upper end of the corresponding interval may therefore provide a preliminary warning reference for abnormalities such as DC magnetic bias, core saturation, and harmonic distortion and may assist in evaluating the transformer excitation state.

The high-to-low frequency-ratio intervals of the acoustic and vibration signals overlap substantially and are markedly higher than those reported for conventional transformers. This difference is associated with the greater magnetostriction of amorphous alloys relative to conventional silicon steel. As the magnetic flux approaches saturation, the flux waveform is more susceptible to distortion and may contain higher-order harmonics [23].

Mechanical looseness of the transformer core or windings, as well as operation under DC magnetic bias, may shift the frequency distribution towards higher frequencies; consequently, the upper end of the high-to-low frequency-ratio interval may serve as a preliminary warning reference. In addition, amorphous alloys exhibit strong nonlinearity and pronounced hysteresis in their magnetostriction curves. Their vibration waveforms therefore contain more aperiodic harmonic components, and the spectral correlation between adjacent time frames is lower. Accordingly, the overall mean autocorrelation degree is lower than that of conventional transformers. A value below the lower end of the reference interval may warrant attention to possible mechanical looseness of the core or windings.

The comparison in Table 4 also shows that the fundamental-frequency-proportion interval is substantially lower than that of conventional transformers. This indicates that, under steady-state operation, the 100 Hz winding-vibration component contributes a smaller proportion of the total spectral energy in this transformer type. DC bias may substantially increase the amplitudes of other frequency components and thereby reduce the fundamental-frequency proportion. The lower end of the distribution interval may therefore be used as a preliminary warning reference.

This study statistically analysed the acoustic and vibration characteristics obtained from factory tests and field measurements of the first 110 kV amorphous-alloy three-dimensional wound-core transformer and established preliminary distribution ranges for its steady-state operating characteristics. Because the investigation was limited to a single prototype and a relatively short operating period, the reported ranges cannot yet be generalized as universal diagnostic thresholds. Future work should include long-term monitoring of the in-service transformer and measurements from additional units under a wider range of operating and fault conditions. Such data will enable continued expansion of the acoustic and vibration sample database and provide more robust technical support for safe operation and maintenance.

4. Conclusions

This study investigated the first 110 kV/20,000 kVA amorphous-alloy three-dimensional wound-core transformer by acquiring acoustic and vibration signals and statistically analysing characteristic quantities under three scenarios: the bare core, the transformer tank wall, and field operation. The acoustic and vibration characteristics were also compared with those of conventional power-frequency transformers. The principal conclusions are as follows:

(1) The principal frequency components of the acoustic and vibration signals from the amorphous-alloy three-dimensional wound-core transformer were even-order harmonics at integer multiples of 100 Hz [20]. The dominant frequency remained primarily at 200 Hz, while a dominant frequency of 300 Hz was observed at some measurement points. The odd-to-even harmonic ratio was considerably lower than that of conventional silicon-steel transformers, demonstrating a more pronounced dominance of even-order harmonics. This ratio may therefore serve as a reference quantity for evaluating abnormal excitation conditions, including DC magnetic bias, core saturation, and harmonic distortion.

(2) The vibration signals measured on the core surface exhibited concentrated mean autocorrelation degrees, low odd-to-even harmonic and high-to-low frequency ratios, and concentrated dominant frequencies. By contrast, vibration signals measured on the tank wall propagated through multiple media, including the core, clamps and insulation, transformer oil, and tank wall, and were additionally affected by differences in transmission paths and assembly tolerances. Consequently, the tank-wall signals exhibited more dispersed dominant frequencies and higher odd-to-even harmonic and high-to-low frequency ratios. When the core was tested separately, without strong constraints from the tank, clamps, and compression structures, the acoustic characteristic quantities showed greater fluctuations and wider distributions. After assembly, the integrated constraints imposed by the clamps, tank, insulation, and compression structures resulted in more concentrated distributions of the acoustic characteristic quantities measured from the transformer body.

(3) The acoustic and vibration characteristic quantities measured at corresponding core and tank-wall positions exhibited a clear positive relationship. Together with the field acoustic and vibration measurements, the results provide preliminary distribution ranges for the characteristic quantities of this transformer type under no-load and light-load operation. These ranges may serve as quantitative baseline references for characteristic evaluation, early fault indication, and field operation, maintenance, and inspection.

References

[1] De Almeida A, Santos B, Martins F. Energy-efficient distribution transformers in Europe: Impact of the Ecodesign Regulation. Energy Efficiency, 2016, 9(2): 401-424.

[2] Maheswaran D, Rangaraj V, Kailas K K J, et al. Energy efficiency in electrical systems. In: 2012 IEEE International Conference on Power

Electronics, Drives and Energy Systems (PEDES). IEEE, 2012: 1-6.

[3] Long Z, Liu J, Chen H. Optimization design of an amorphous-alloy core transformer. Automation of Electric Transmission, 2019, 46(1): 68-71, 55.

[4] Liu J. Study on the generation mechanism of core fragments in amorphous-alloy transformers and their influence on insulation. Electronic Measurement Technology, 2022, 45(19): 44-49.

[5] Ma F, Niu D, Han C. Application prospects of amorphous-alloy transformers in railway power-supply systems. Journal of Railway Engineering, 2014, 31(11): 94-97.

[6] Zheng G, Liu Z, Chen X, et al. Technical and economic analysis of SH15 amorphous-alloy core distribution transformers. Transformer, 2005, 42(6): 1-5.

[7] Ng H W, Hasegawa R, Lee A C, et al. Amorphous-alloy core distribution transformers. Proceedings of the IEEE, 1991, 79(11): 1608-1623.

[8] Li X, Wen X, Markham P N, et al. Analysis of nonlinear characteristics for a three-phase, five-limb transformer under DC bias. IEEE Transactions on Power Delivery, 2010, 25(4): 2504-2510.

[9] Song W, et al. Magnetostrictive vibration characteristics of an amorphous-alloy transformer with a three-dimensional wound core. IEEE Access, 2024, 12: 43958-43967.

[10] Du B X, Liu D S. Dynamic behavior of magnetostriction-induced vibration and noise of amorphous-alloy cores. IEEE Transactions on Magnetics, 2014, 51(4): 1-8.

[11] Weiser B, Pfützner H, Anger J. Relevance of magnetostriction and forces to the generation of audible noise in transformer cores. IEEE Transactions on Magnetics, 2000, 36(5): 3759-3777.

[12] Shilyashki G, Pfützner H, Hamberger P, et al. Spatial distributions of magnetostriction, displacement, and noise generation in model transformer cores. International Journal of Mechanical Sciences, 2016, 118: 188-194.

[13] Wang B. Acoustic fingerprint diagnostic technology for typical operating conditions of power transformers. North China Electric Power University (Beijing), 2022. DOI: 10.27140/d.cnki.ghbbu.2022.000055.

[14] Bartoletti C, Desiderio M, Di Carlo D, et al. Vibro-acoustic techniques to diagnose power transformers. IEEE Transactions on Power Delivery, 2004, 19(1): 221-229. DOI: 10.1109/TPWRD.2003.820177.

[15] Rikardo S A, Bambang C B, Sumaryadi C, et al. Vibration monitoring of power transformers. In: 2008 International Conference on Condition Monitoring and Diagnosis. IEEE, 2008: 1015-1016.

[16] García B, Burgos J C, Alonso Á M. Transformer tank vibration modeling as a method for detecting winding deformations-Part I: Theoretical foundation. IEEE Transactions on Power Delivery, 2006, 21(1): 157-163. DOI: 10.1109/TPWRD.2005.852280.

[17] Belahcen A. Vibrations of rotating electrical machines due to magnetomechanical coupling and magnetostriction. IEEE Transactions on Magnetics, 2006, 42(4): 971-974. DOI: 10.1109/TMAG.2006.871469.

[18] Miao X, Jiang P, Pang F, Tang Y, Li H, Qu G, et al. Numerical analysis and experimental investigation of the vibration and noise characteristics of oil-immersed power transformers. Applied Acoustics, 2023, 203: 109189. DOI: 10.1016/j.apacoust.2022.109189.

[19] Liu Y, Li L, et al. Simulation and experimental study of vibration in an amorphous-alloy three-dimensional wound core considering magnetostriction. Advanced Technology of Electrical Engineering and Energy, 2022, 41(3): 15-22.

[20] Chen Z, Du Z, Xiang Y, et al. Study on acoustic-vibration coupling of a magnetically controlled distribution transformer considering DC bias. Electric Power Systems Research, 2026, 253: 112544.

[21] Zhang S J. Research on detection and diagnostic technology for the acoustic-vibration characteristics of low-frequency power transformers. North China Electric Power University, 2025. DOI: 10.27139/d.cnki.ghbdu.2025.002236.

[22] Liu Y, Wang B, Zhou X, et al. Determination of early-warning thresholds for acoustic fingerprint characteristics based on 162 ultra-high-voltage and extra-high-voltage transformers. Journal of North China Electric Power University (Natural Science Edition), 2021, 48(5): 45-53.

[23] Han X, Song W, Liu Y, et al. Analysis of the magnetostriction, vibration, and noise characteristics of transformer cores made of different ferromagnetic materials. Large Electric Machine and Hydraulic Turbine, 2023, (1): 68-73.

[24] Song W, Han Y, Yang F, et al. Magnetostrictive vibration characteristics of an amorphous-alloy transformer with a three-dimensional wound core. IEEE Access, 2024, 12: 43958-43967.